IAC-19-C2.6.2

Electrodynamic Dust Shield Testing on the Materials on International Space Station Experiment 11

Michael R. Johansen[†a*], Michael A. Dupuis[‡b], James R. Phillips III[†c], Joel D. Malissa[†d], Jerry J. Wang[†e], Michael D. Hogue[†f], Carlos I. Calle[†g]

[†] *Spaceport Technologies Office, NASA KSC Mailcode UB-G, Kennedy Space Center, FL 32899*
[‡] *Advanced Engineering Development Branch, NASA KSC Mailcode NE-L6, Kennedy Space Center, FL 32899*

[a] michael.r.johansen@nasa.gov; [b] michael.a.dupuis@nasa.gov; [c] james.r.phillips.iii@nasa.gov; [d] joel.d.malissa@nasa.gov; [e] jerry.j.wang@nasa.gov; [f] michael.d.hogue@nasa.gov; [g] carlos.i.calle@nasa.gov;
[*] Corresponding Author

Abstract

Dust is a major concern for lunar exploration. To combat the effects of dust, NASA, academia, and industry are developing solutions to the dust problem. One potential technology solution for this problem is the Electrodynamic Dust Shield (EDS). Many years of research and development have gone into this technology. The Materials on International Space Station Experiment – 11 (MISSE-11) provides a long term space exposure platform for this technology to verify compatibility of materials and manufacturing processes to the space environment. The MISSE-11 EDS experiment consists of 12 EDS panels. These panels are made of glass, polyimide, or prototype spacesuit fabric. Some panels are covered with a lotus leaf coating while others are covered with thermal paint. They are flown in the wake position of the ISS to simulate the lunar environment. Two panels are in an active configuration and are energized with a high voltage power supply, which generates high-voltage pulses to activate the dust shields. Current and voltage data are recovered from each of these trials to compare to baseline data. Also, each of the EDS panels are imaged on a monthly basis to track any changes with time that may occur with the EDS variants. In this paper, we report preliminary data and analysis from this spaceflight experiment.

Keywords: Electrodynamics, Lunar, Dust, ISS, MISSE

1. Introduction

From the Commercial Lunar Payload Services (CLPS) missions to the Artemis program's goal to return humans to the moon in 2024, NASA's current commitment to lunar exploration is unprecedented since the closeout of the Apollo program in the early 1970s. The Apollo program taught us a great deal about the challenges awaiting our return as we contemplate wider ranging robotic exploration, resource identification, extraction, and utilization, and longer duration human habitation on the lunar surface. And one of the major challenges impacting all future lunar surface missions, the Apollo program showed us, is dust.

Lunar dust is pervasive. It is easily mobilized or "kicked up" by rover wheels, digging tools, astronaut boots, rocket exhaust plumes, etc. These same actions will also electrostatically charge dust particles, causing them to adhere to nearly all surfaces, with obvious deleterious effects to solar panels, astronaut visors, and camera lenses, to name a few. Lunar dust can also be extremely fine-grained and abrasive, allowing it to migrate into and foul mechanical and electro-mechanical systems such as gearboxes, actuator motors, wheel hubs, mechanical joints, and airlock seals. The impact of lunar dust was succinctly summarized by the Dust Mitigation Gap Assessment Team in their 2016 Final Report [1]:

> "Dust is still a principal limiting factor in returning to the lunar surface for missions of any extended duration. However, viable technology solutions have been identified, but need maturation to be available to support both lunar and Mars missions."

In April 2019, the EDS experiment was launched to the International Space Station (ISS) for space environment testing. This technology was developed by scientists, engineers, and supporting personnel at NASA's Kennedy Space Center (KSC) Electrostatics and Surface Physics Laboratory (ESPL), and represents the latest step in years of EDS research and technology development by the KSC's ESPL. The EDS is currently stationed on the Materials ISS Experiment – Flight Facility (MISSE-FF), an ISS external structure housing experiments that require exposure to a space environment. The EDS, described in detail below, will be returned to KSC after spending approximately 12 months on-orbit.

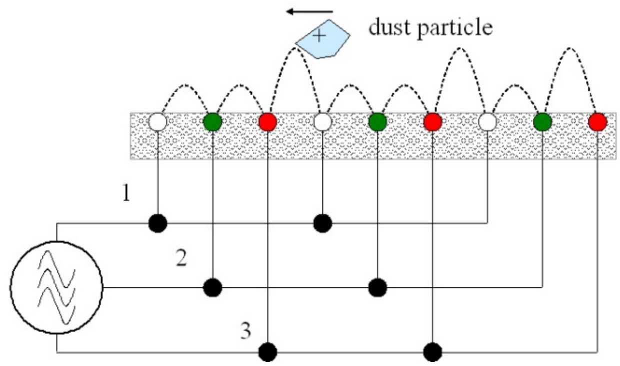

Figure 1: Schematic operation of the EDS [3].

1.1 *Electrodynamic Dust Shield Physics*

The Apollo missions showed that the dry, powdery dust on the lunar surface not only adheres mechanically due to its jagged morphology, but also adheres to surfaces via electrostatics and Van Der Waals forces [2]. Dust adhesion to critical surfaces such as joints, seals, and spacesuit visors created issues for the Apollo astronauts that need to be addressed prior to a return to the Moon for sustained operations.

At KSC, the ESPL has been developing an electrodynamic dust removal technology that uses non-uniform electric fields known as the EDS [3]. These non-uniform fields create a traveling electrodynamic wave across the surface that moves adherent dust particles via the dielectrophoretic (DEP) force [4]. The DEP force is given by

$$\vec{F}_{\text{DEP}} = 2\varepsilon_0\varepsilon_1 K r^3 \vec{\nabla} E^2 \tag{1}$$

where E is the electric field, r is the particle radius, ε_0 and ε_1 are the electrical permittivities of free space and dust, respectively, and K is the Clausius – Mossotti function given by

$$K = \frac{\varepsilon_2 - \varepsilon_1}{\varepsilon_2 + 2\varepsilon_1} \tag{2}$$

where ε_2 is the electrical permittivity of the medium. A schematic of the operation of a three-phase EDS is shown in Figure 1.

The ESPL has, over a period of ten years, developed various types of the EDS to fit various requirements for dust mitigation. The EDS technology is extensively tested in the ESPL with lunar simulants, sands, powders, etc., and with actual lunar dust brought back from the Apollo missions. These experiments are performed in vacuum chambers to simulate the lunar environment. Experiments conducted on several reduced gravity flights to simulate lunar gravity and vacuum conditions with both lunar regolith simulants and Apollo regolith samples were successful.

2. Experiment Design

2.1 *Materials Design*

The EDS Experiment for MISSE-11 was designed to expose different implementations of the EDS system to the low-Earth-orbit space environment. Two systems, an EDS for optical systems and an EDS for thermal radiators were connected to two high voltage power supplies. These active EDS panels were controlled through a Data Communications unit and programmed to operate several times per day. The ten additional EDS systems were not connected to power supplies while on orbit. These passive EDS panels will be operated in a vacuum chamber at the end of the MISSE-11 experiment, when the samples return to our laboratory.

The design of the active EDS for optical systems uses two-phase indium tin oxide (ITO) interdigitated electrodes on a 50 mm x 50 mm x 0.7 mm boro-aluminosilicate glass. A cover glass 0.2 mm thick was positioned over the electrodes using a high dielectric adhesive. The samples are enclosed in a frame with a Teflon base and an aluminum front.

The passive samples include duplicates of the two active samples, an EDS for flexible thermal radiators with aluminum electrodes on fluorinated ethylene propylene (FEP), and four EDS panels for thermal radiators with a nano-textured coating with hydrophobic properties from NASA Goddard Space Flight Center. Two of these EDS panels were painted with AZ-93 thermal paint. An EDS for spacesuits with conductive ink electrodes screen-printed on a Technora/Polybenzobisoxazole fabric (Honeywell Millenia XT) from the University of South Dakota was also included. Finally, we included two 50 mm x 75 mm x 1.1 mm EDS panels for optical systems with ITO electrodes on boro-aluminosilicate glass. One of these two EDS panels has a tantalum pentoxide dielectric coating over the electrode pattern and the second one has an antireflective dielectric coating. Table 1 summarizes the main properties of the twelve EDS panels on the MISSE experiment. Figure 2 shows the samples mounted on the MISSE experiment carrier.

2.2 *Electronics Design*

In the flight configuration shown in Figure 3, the MISSE Sample Carrier (MSC) interfaces with the Data Communications Unit (DCU) over an RS-422 serial bus and enables the internal microcontroller unit (MCU) and analog to digital converter (ADC) of the DCU via digital inputs. The MSC provides a nominal $28\,\text{V}$ supply to the DCU which further regulates its input power down to $24\,\text{V}$ to pass along to the two connected high voltage power supply (HVPS) modules. Each of these two HVPS modules is interfaced with a corresponding EDS module to which it provides a $4\,\text{kV}$ amplitude, $10\,\text{Hz}$ frequency square wave signal when enabled. The HVPS

Table 1: Active and passive samples on the EDS Experiment for MISSE-11

Type	**EDS Technology**	**Coating**	**Area** (mm^2)
Active	ITO electrodes on boro-aluminosilicate glass	Cover glass (200 µm)	50 × 50
Active	Copper electrodes on Kapton film	Kapton	50 × 50
Passive	ITO electrodes on boro-aluminosilicate glass	Cover glass (200 µm)	50 × 50
Passive	Copper electrodes on Kapton film	Kapton	50 × 50
Passive	Aluminum electrodes on FEP film	None-FEP space facing	50 × 50
Passive	Copper electrodes on Kapton film	Kapton/nano-textured	50 × 50
Passive	Copper electrodes on Kapton film	Kapton/nano-textured	50 × 50
Passive	Copper electrodes on Kapton film with Z-93 paint	Kapton/nano-textured	50 × 50
Passive	Copper electrodes on Kapton film with Z-93 paint	Kapton/nano-textured	50 × 50
Passive	Millenia XT electrodes on Technora/PBO fabric	None	50 × 50
Passive	ITO electrodes on boro-aluminosilicate glass	Tantalum pentoxide	50 × 75
Passive	ITO electrodes on boro-aluminosilicate glass	Abrisa BBAR-399	50 × 75

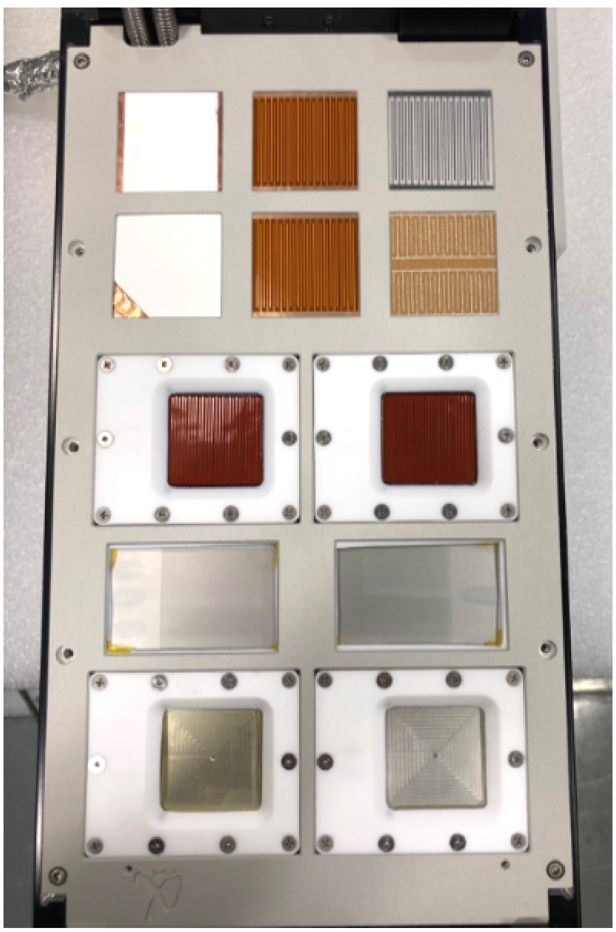

Figure 2: Active and passive samples for the EDS experiment on MISSE-11.

modules generate a pulsed heartbeat signal aligned with the state changes of the high voltage waveform output to the EDS modules. Due to increased complexity and time constraints, the design of the DCU did not allow for monitoring of this heartbeat signal, so frequency measurements cannot be taken. The ADC within the DCU monitors and logs output voltage and current to each HVPS module at a frequency of 5000 samples per second so that anomalies in operation may be detected.

In the ground configuration (not shown), the MSC is replaced by a benchtop power supply to provide the requisite 28 V input to the DCU and the MCU and ADC enable signals are provided via physical switches. Communication with the DCU is done by directly interfacing via secure shell to the MCU over Ethernet rather than providing commands over the RS-422 protocol. All other operation is identical to flight.

2.3 Experimental Data

Prior to delivery for launch, the flight DCU as well as the two flight HVPS modules with associated EDS panels were installed within a high vacuum belljar to simulate the conditions expected outside of ISS. Bus A of the DCU was configured with a Kapton EDS panel and bus B was configured with a glass EDS panel. The setup was operated as it would be on orbit: high voltage waveforms applied to the EDS panels for one minute each hour. To avoid overstressing the flight units so close to the delivery date, only five repetitions were completed to ensure nominal operation. Figure 4 shows the entire voltage and current waveform for each bus during the first of these runs, while Figure 5 displays a summary of all of the runs.

Stress testing was performed on the ground DCU and HVPS modules to evaluate their robustness. To ensure any detected failure would not be a function of the EDS panel in use, an idealized capacitive load was substituted for the panel. Figure 6 shows the entire voltage and current waveform for each bus during the first of these runs. A representative sample of forty of these tests are shown in Figure 7 where each bus was operated for one minute every ten minutes for forty repetitions. Preliminary results show that the DCU returned consistent voltage and current measurements over this time period.

Mean current draw of the HVPS module as measured by the DCU is typically between 69 and $73\,\mathrm{mA}$ when an EDS module is used as the load (as seen in Figures 4, 5, 8, and 9). The standard deviation of this current if under $8\,\mathrm{mA}$ under normal operation (note the exception of bus A in Figures 8 and 9). When the capacitive load is used in place of an EDS module, both the mean and deviation of the current is significantly increased to nearly $90 \pm 25\,\mathrm{mA}$ (as seen in Figures 6 and 7). This is most likely due to the capacitance of the simulated load being much higher than the capacitance of the EDS modules in use.

The two data sets acquired from the experiment on orbit are shown in Figures 8 and 9. During the first run on ISS (Figure 8), more than fifteen current spikes (and their corresponding voltage dips) were detected on bus A controlling the Kapton EDS panel. The cause of this anomaly is unknown. The glass EDS panel installed on bus B behaved similarly to the tests on the ground in the vacuum chamber (Figure 4). The second run on orbit (Figure 9) shows a single current spike on bus A and nominal operation on bus B.

2.4 Preflight Ground Testing

Several non-flight EDS panels and an HVPS module underwent vibrational and thermal vacuum preflight testing. To simulate launch conditions, the vibration tests performed at the KSC Vibration Test Facility such as the three shown in Figure 10 used the test parameters listed in Table 2 for an HVPS, Cu-Kapton shield, and glass shield. All EDS panels tested cleared dust nominally before and after vibration testing, no cracks were visible to the naked eye in the glass EDS, and the current draw of the HVPS module was similarly nominal after this testing.

In addition to vibration testing, the final Cu-Kapton EDS, glass EDS, and HVPS test units passed extensive thermal testing in the ESPL's thermal vacuum chamber (Figure 11) constructed for these tests, which uses an oil-regulated cold plate for fine temperature control thermally bonded to a liquid-nitrogen-regulated cold plate for coarse temperature control. The tests simulated prolonged hot and cold unpowered storage in vacuum conditions during preflight checkouts and powered operations in orbital temperature extremes. Table 2 lists the thermal testing parameters. Figure 12 photographed early failures with electrical breakdowns across debonded surfaces or through thin dielectric volumes, both of which were resolved with more insulating material. Additionally, extended duration testing with thermocouples on the high voltage DC-DC converter and low voltage regulator found that the high voltage converter experiences the greatest temperature rise during continuous use beyond the duration of active tests. (Figure 13) The final EDS tests cleared dust nominally before and after all thermal testing. The current draw monitored on an oscilloscope during powered testing was reviewed and accepted with $30\,\mu\mathrm{s}$, off-nominal bursts up to $700\,\mathrm{mA}$ because their short duration did not inhibit performance.

3. Conclusion

The EDS dust mitigation system is currently under consideration for use by CLPS payloads and landers and also the Artemis program. Results from this demonstration will inform NASA on the readiness of this technology to be infused into these programs.

Preliminary results and photos indicate that the EDS hardware is performing nominally. The hardware will return in April 2020, after spending one year exposed to the space environment. The active and passive samples will undergo testing to determine the effect the space environment has on the EDS system.

References

[1] Dust Mitigation Gap Assessment Team *Dust Mitigation Gap Assessment Report.* International Space Exploration Coordination Group, 2016.

[2] O.R. Walton. *Adhesion of lunar dust.* NASA/CR–2007-214685.

[3] C.I. Calle, C.R. Buhler, M.R. Johansen, M.D. Hogue, S.J. Snyder. *Active dust control and mitigation technology for lunar and Martian exploration.* Acta Astronautica, 69 (2011) 1082 – 1088.

[4] J.A. Cross. *Electrostatics: Principles, Problems, and Applications.* Hilger, Bristol, 1987.

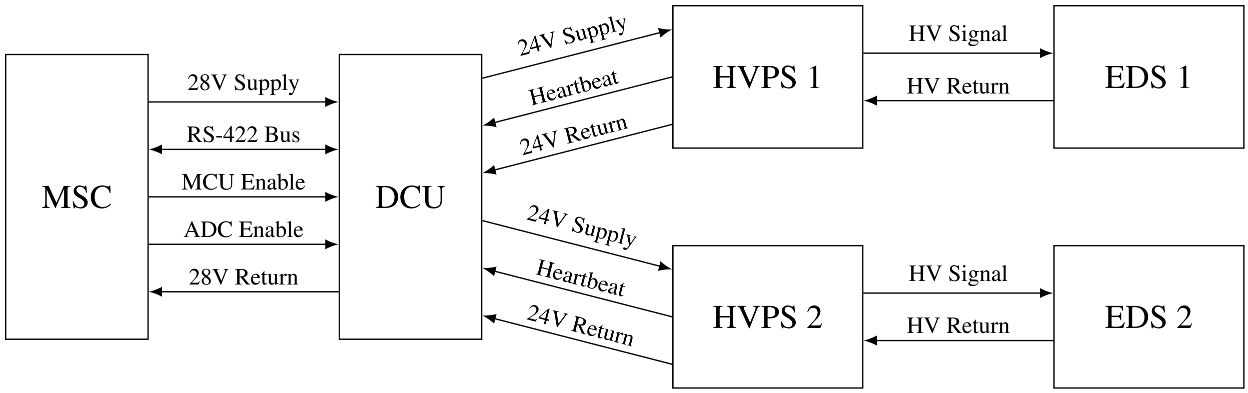

Figure 3: Configuration of EDS experiment for flight on ISS.

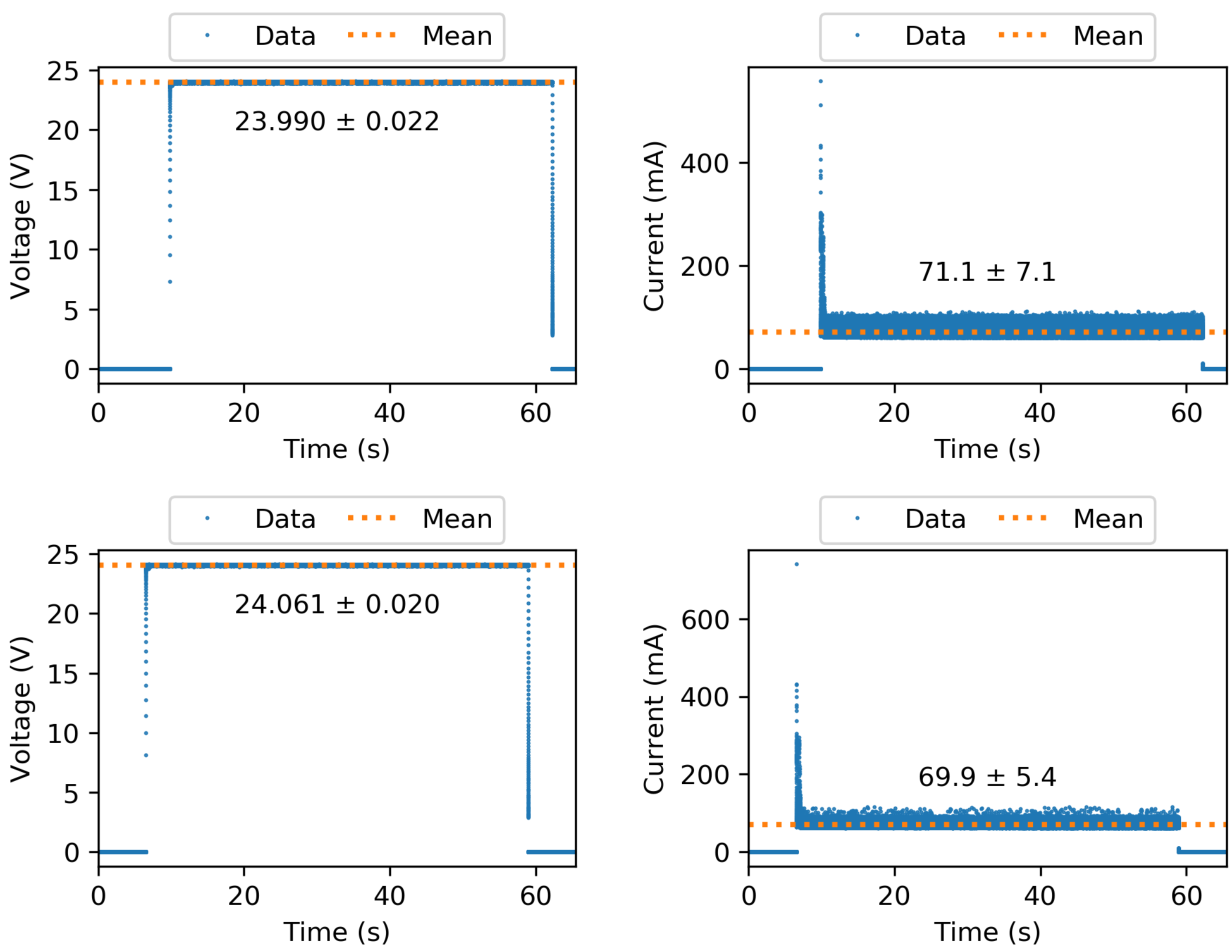

Figure 4: HVPS input voltage (left) and current (right) waveforms from first ground test of flight DCU with Kapton EDS installed on bus A (top) and glass EDS installed on bus B (bottom) before delivery for launch.

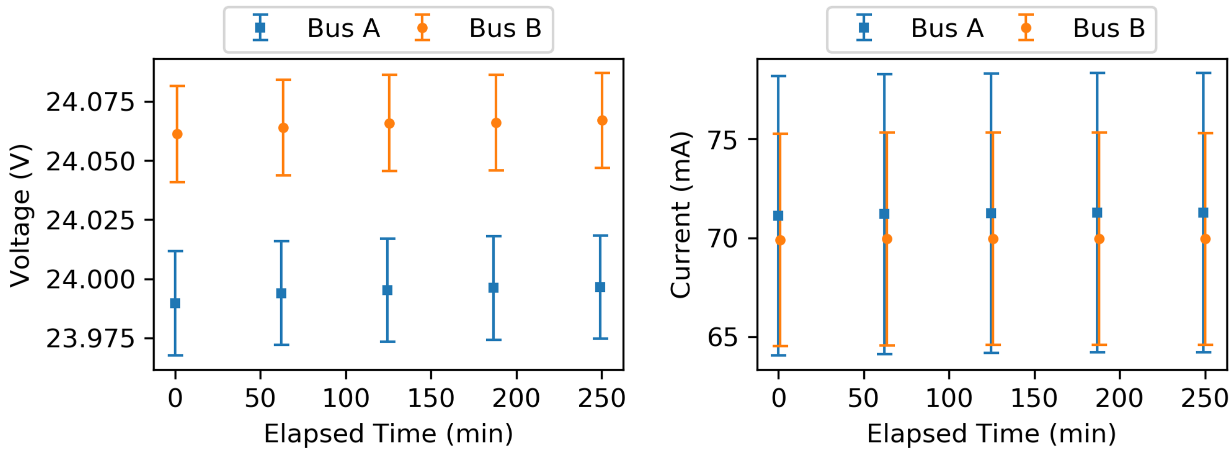

Figure 5: Mean voltages (left) and currents (right) from subsequent ground tests of flight DCU at hourly intervals with Kapton EDS on bus A and glass EDS on bus B loads before delivery for launch.

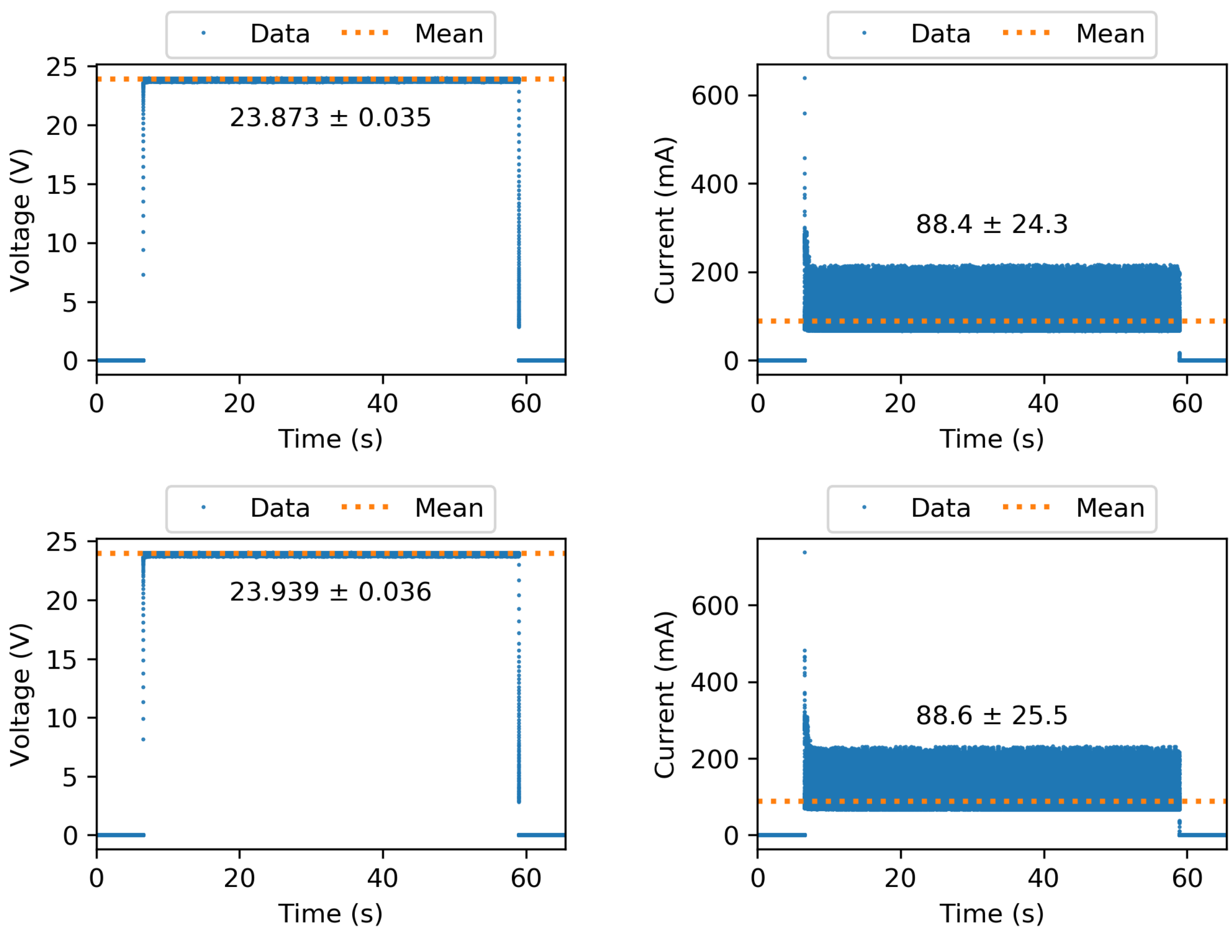

Figure 6: HVPS input voltage (left) and current (right) waveforms from first run of ground DCU stress testing with capacitive loads installed on both buses.

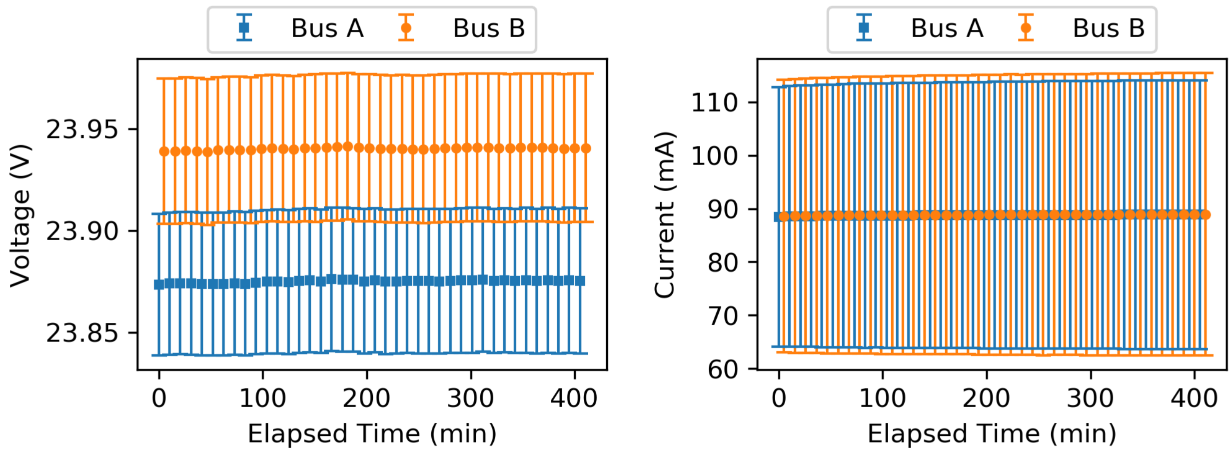

Figure 7: Mean voltages (left) and currents (right) from subsequent runs of ground DCU stress testing at ten minute intervals with capacitive loads installed on both buses.

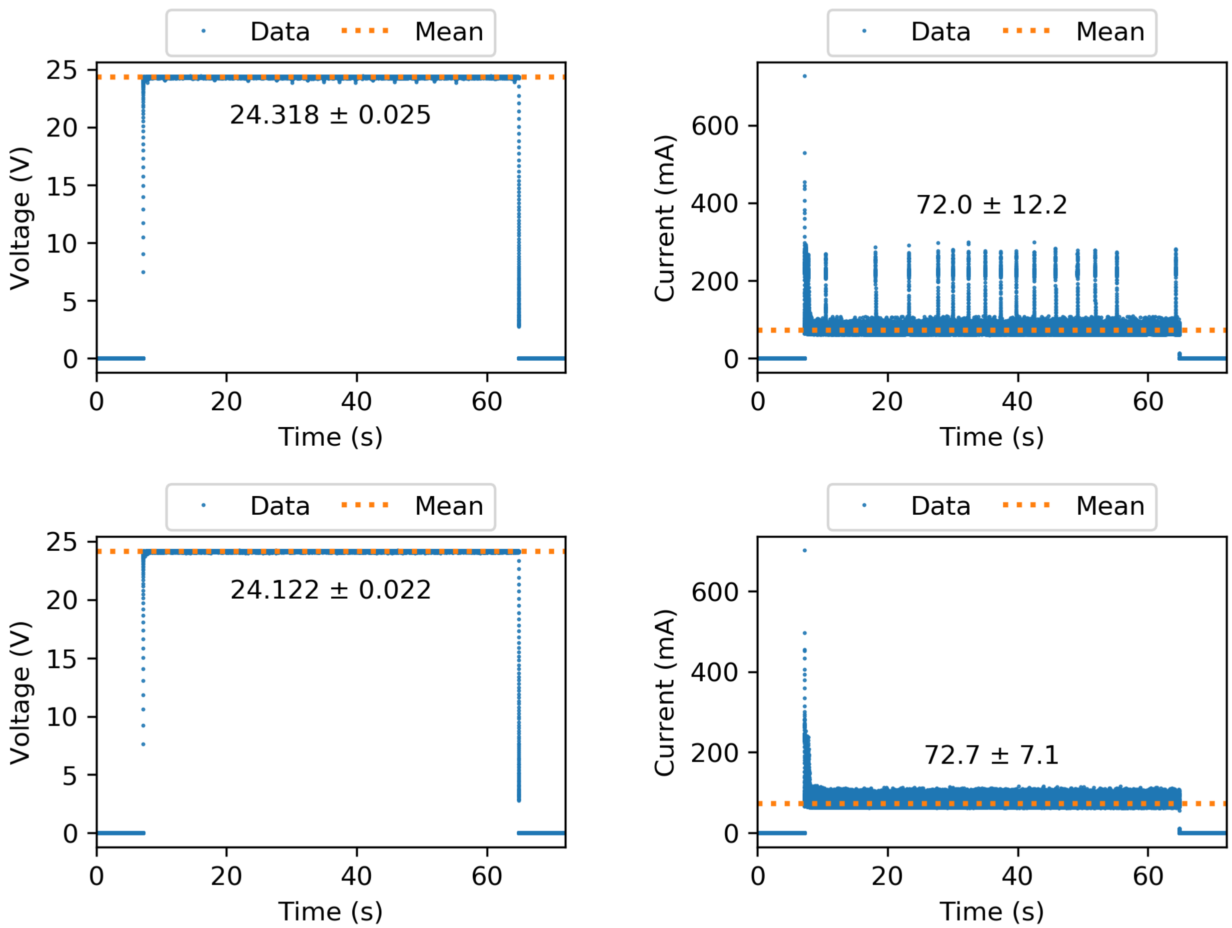

Figure 8: HVPS input voltage (left) and current (right) waveforms from first flight test with Kapton EDS installed on bus A (top) and glass EDS installed on bus B (bottom) of DCU.

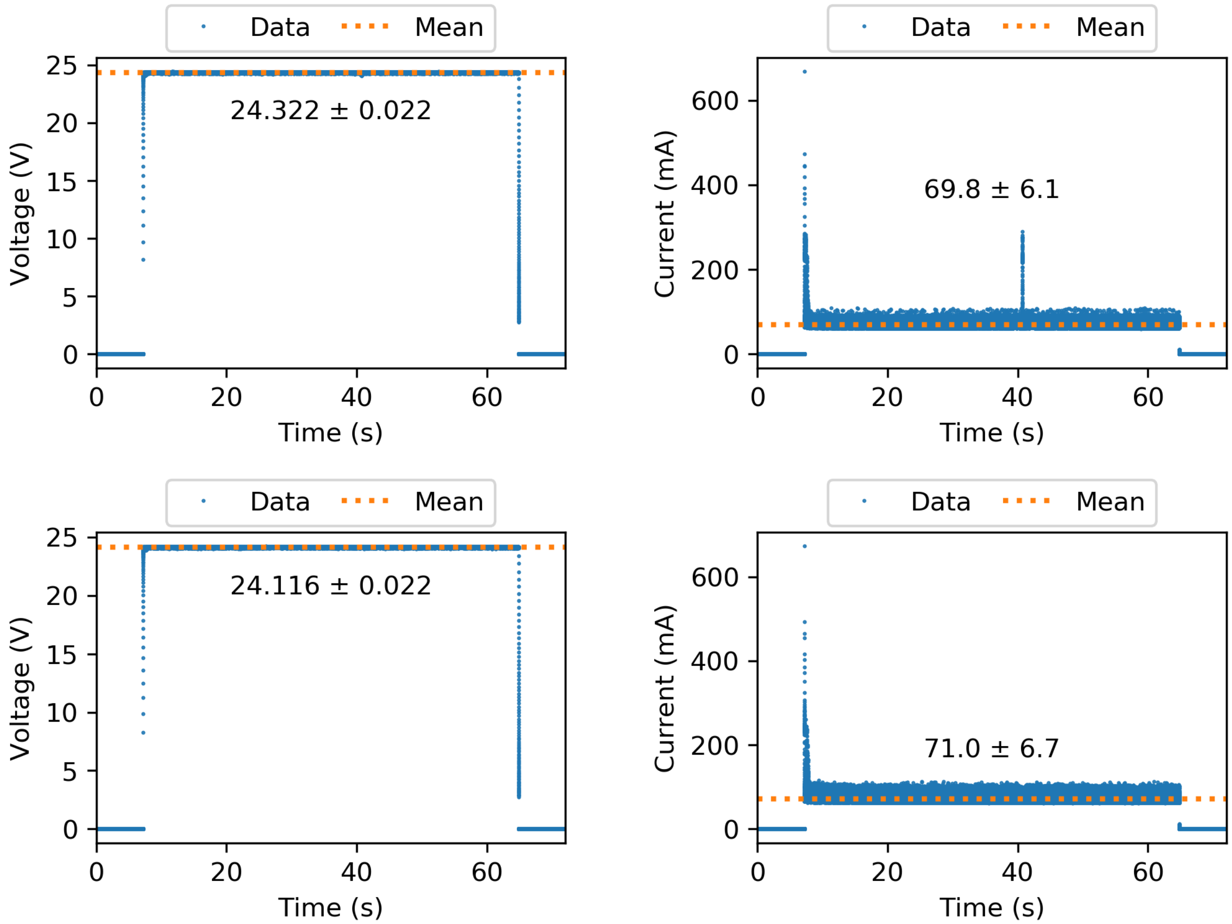

Figure 9: HVPS input voltage (left) and current (right) waveforms from second flight test with Kapton EDS installed on bus A (top) and glass EDS installed on bus B (bottom) of DCU.

Table 2: Ground environmental testing requirements.

Environment	**Test**	**Parameter**	**Value**
Vibration		Frequency Sweep	20 - 2000 Hz
		Acceleration (RMS)	8.8 g
		Duration	1 min
Thermal Vacuum	Cold Storage	Temperature	$-40\,^{\circ}$C
		Duration	90 min
		Pressure	3×10^{-5} Torr
	Hot Storage	Temperature	$60\,^{\circ}$C
		Duration	90 min
		Pressure	3×10^{-5} Torr
	Powered	Temperature	$0, 5, \ldots, 40, 45\,^{\circ}$C (10 trials)
		Duration	1 min at each temperature
		Pressure	3×10^{-5} Torr

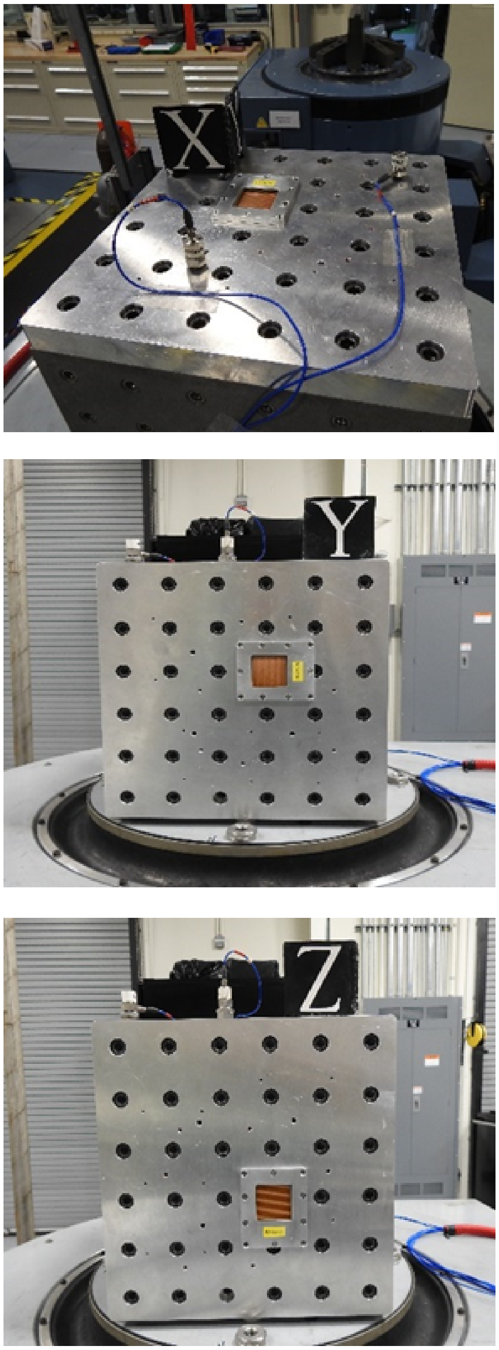

Figure 10: Cu-Kapton EDS vibration tests
(HVPS and glass EDS vibration tests not shown).

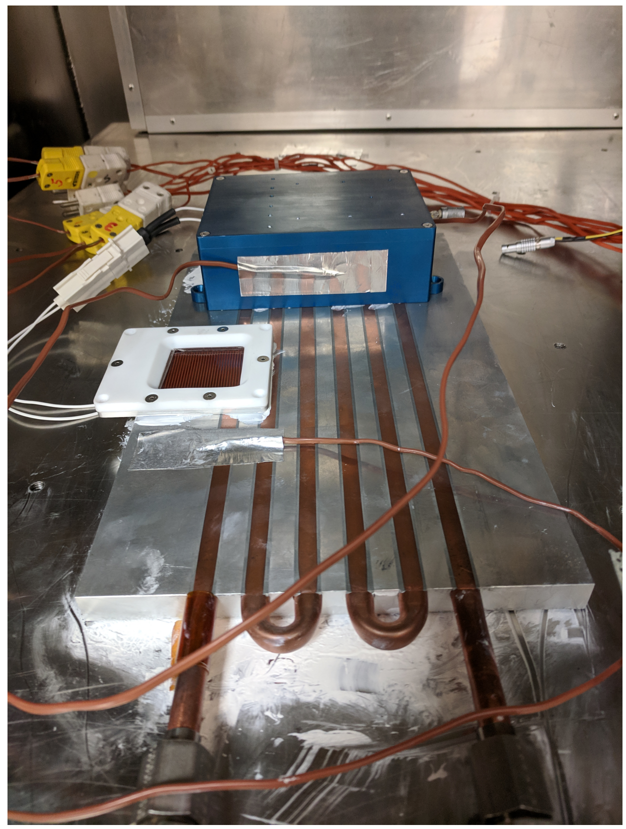

Figure 11: Thermal vacuum chamber.

Figure 12: Arcing across a debonded surface (left) and through a thin dielectric (right)

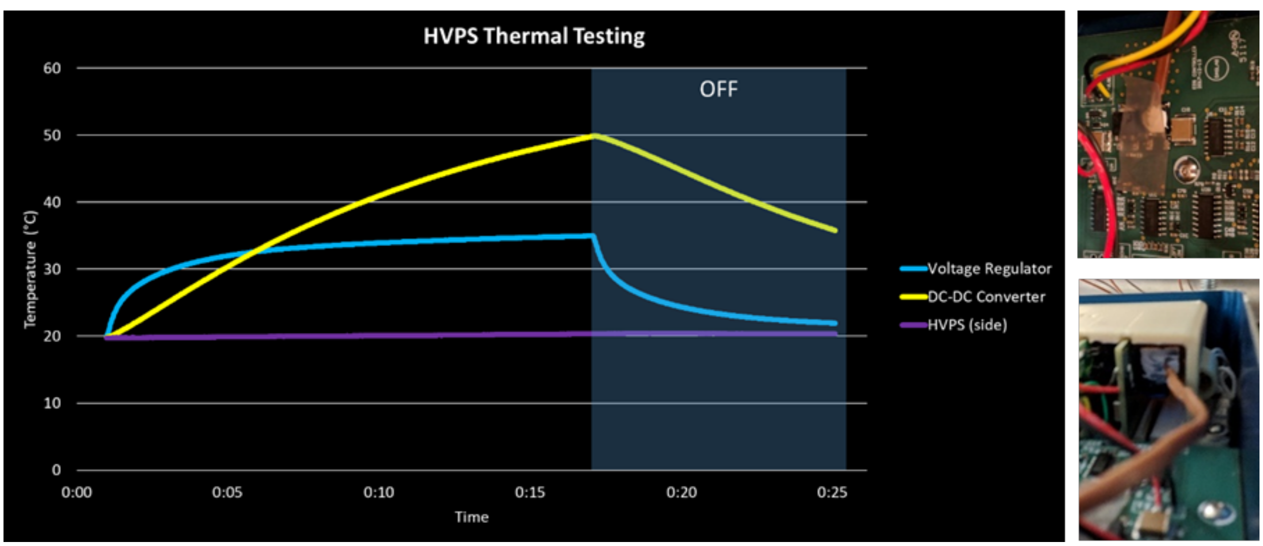

Figure 13: Extended HVPS testing results (left) with thermocouples mounted to the low voltage regulator (upper right) and high voltage converter (lower right).